Biochimica et Biophysica Acta 1864 (2017) 355–366

https://doi.org/10.1016/j.bbamcr.2016.11.022

Mitochondrial cAMP prevents apoptosis modulating Sirt3 protein level and OPA1 processing in cardiac myoblast cells

Anna Signorile [a,*,1], Arcangela Santeramo [a], Grazia Tamma [b], Tommaso Pellegrino [b], Susanna D'Oria [c], Paolo Lattanzio [d],Domenico De Rasmo [d,1]

a Department of Basic Medical Sciences, Neurosciences and Sense Organs, University of Bari "Aldo Moro",Bari 70124, Italy b Department of Bioscience, Biotechnologies and Biopharmaceutics, University of Bari "Aldo Moro", Bari 70125, Italy Department of Biomedical Sciences and Human Oncology, University of Bari "Aldo Moro",Bari 70124, Italy d Institute of Biomembrane and Bioenergetics, CNR, Bari 70124, Italy

article info abstract

Article history:
Received 10 June 2016 Received in revised form 3 November 2016 Accepted 23 November 2016 Available online 24 November 2016

Keywords:
Mitochondria cAMP Apoptosis Sirt3 OPA1

Abbreviations: 8-Br-cAMP, 8-Bromoadenosine 3′,5′-cyclic monophosphate; 8pCPT, 8pCPT-2′-O-Me-cAMP; cAMP, 3′,5′-cyclic adenosine monophosphate; DRP-1, Dynamin related protein 1; Epac, exchange protein directly activated by cAMP; L-OPA, long OPA1; OPA1, optic atrophy 1; PKA, protein kinase A; ROS, reactive oxygen species; sAC, soluble adenylyl cyclase; S-OPA, short OPA1; t-BHP, tert-butyl hydroperoxide; tmAC, transmembrane adenylyl cyclase.

∗ Corresponding author at: Department of Basic Medical Sciences, Neurosciences and Sense Organs, University of Bari "Aldo Moro", Policlinico, P.zza G. Cesare, 11, 70124 Bari, Italy.

E-mail address: anna.signorile@uniba.it (A. Signorile).

Mitochondria, responding to a wide variety of signals, including oxidative stress, are critical in regulating apoptosis that plays a key role in the pathogenesis of a variety of cardiovascular diseases. A number of mitochondrial proteins and pathways have been found to be involved in the mitochondrial dependent apoptosis mechanism, such as optic atrophy 1 (OPA1), sirtuin 3 (Sirt3), deacetylase enzyme and cAMP signal. In the present work we report a network among OPA1, Sirt3 and cAMP in ROS-dependent apoptosis. Rat myoblastic H9c2 cell lines, were treated with tert-butyl hydroperoxide (t-BHP) to induce oxidative stress-dependent apoptosis. FRET analysis revealed a selective decrease of mitochondrial cAMP in response to t-BHP treatment. This was associated with a decrease of Sirt3 protein level and proteolytic processing of OPA1. Pretreatment of cells with permeant analogous of cAMP (8-Br-cAMP) protected the cell from apoptosis preventing all these events. Using H89, inhibitor of the protein kinase A (PKA), and protease inhibitors, evidences have been obtained that ROS-dependent apoptosis is associated with an alteration of mitochondrial cAMP/PKA signal that causes degradation/proteolysis of Sirt3 that, in turn, promotes acetylation and proteolytic processing of OPA1.

1. Introduction

Apoptosis plays a key role in the pathogenesis of cardiovascular diseases. Cardiac myocytes undergoing apoptosis have been identified in tissue samples from patients suffering from myocardial infarction, diabetic cardiomyopathy, and end-stage congestive heart failure. Notably, apoptosis inhibition is cardio-protective under many conditions. Apoptosis is activated in cardiac myocytes by multiple stressors, commonly seen in cardiovascular diseases, such as cytochine production [1],DNA damage [2] and oxidative stress [3]. Oxidative stress has been associated with loss of cells in cardiac diseases [4] and, on the other hand, increased generation of reactive oxygen species (ROS) was associated with mitochondrial dysfunction [5,6] and apoptosis [7]. Mitochondria play a main role in both life and death of cardiac myocytes. Their primary function is to provide ATP, through oxidative phosphorylation, depending on the energy demand of the beating heart. At the same time, mitochondria are sensible to oxidative stress and are critical in regulating apoptosis responding themselves to a wide variety of stress signals. Many of mitochondrial proteins have been found to be involved in mitochondrial induced apoptosis and are commonly used as targets for studying apoptosis [4]. Recently, other proteins and signals have been found to be involved in the mitochondrial dependent apoptosis mechanism, such as optic atrophy 1(OPA1) [8,9], sirtuin 3 (Sirt3) deacetylase enzyme [10] and 3′,5′-cyclic adenosine monophosphate (cAMP) signal [11].

OPA1 is a conserved GTPase of the dynamin family that mediate mitochondrial fusion and fission. Loss of OPA1 impairs mitochondrial fusion, perturbs cristae structure, and increases the susceptibility of cells toward apoptosis [8]. During apoptosis an alteration of mitochondrial morphology has been observed associated with deregulation of OPA1 and dynamin-related protein 1 (DRP-1), two proteins involved in the balance of mitochondrial fission/fusion [12,13]. A decrease of OPA1 and an increase in small mitochondria are reported in vivo models of heart failure [14]. OPA1 also undergoes constitutive processing leading to the conversion of the uncleaved long OPA1 (L-OPA) in a cleaved short OPA1 (S-OPA) form. Various stress conditions, including apoptotic stimulation, trigger the complete conversion of L.-OPA1 into S-OPA1 [15]. Two mitochondrial proteases, OMA1 and YMEL1 cleave OPA1 from L to S form [16] and their activity is regulated by reciprocal degradation to adapt mitochondrial function to specific cellular stress [17].

Sirt3 is a major mitochondrial deacetylase, that not only modulates cellular metabolism by deacetylation of enzymes involved in fatty acid β-oxidation, amino acid metabolism, electron transport chain, and antioxidant defenses, but also plays an important role in apoptosis [18], tumor growth [19],aging [20] and cardiac diseases [10].Sirt3 prevents apoptosis by lowering ROS and inhibiting components of the mitochondrial permeability transition pore.

cAMP is a ubiquitous second messenger critically involved in the regulation of heart function [21] and many other cellular process including mitochondrial homeostasis [22–25]. In mammalian cells, cAMP can be generated by two distinct form of adenylyl cyclase: a family of transmembrane adenylyl cyclase (tmAC) and soluble adenylyl cyclase (sAC) that produces cAMP in different intracellular microdomains including

mitochondria [25]. Previous works have shown that the activation of cytosolic pathway of cAMP/PKA increases the activity of the respiratory chain complex I [5,6,26] and sAC-dependent cAMP production in mitochondria promotes cytochrome c oxidase activity [27],ATP production [23,28], the turnover of nuclear-encoded subunits of complex I and its activity [29] and regulates the functional activity and structural organization of F_0F_1 ATP synthase [28]. The cAMP signaling pathway also plays an essential role in modulating the apoptotic response to various stimuli and changes of cellular cAMP level can lead to induction or suppression of apoptosis depending on cell types [30–33].

Here a network among mitochondrial cAMP, Sirt3 and OPA1 in ROS-dependent apoptosis in cardiac myoblast cells is reported. Apoptosis was induced in the rat myoblastic H9c2 cell line, widely used as a surrogate for cardiac cells [34], by treatment with tert-butyl hydroperoxide (t-BHP). The results show that increased ROS trigger apoptosis mechanism associated with a decrease of mitochondrial cAMP, Sirt3 protein level and OPA1 proteolytic processing. All these effects were prevented by 8-Br-cAMP. Using H89, inhibitor of the protein kinase A (PKA), and protease inhibitors, evidences have been obtained that, in ROS-induced apoptosis in cardiac myoblasts, an alteration of mitochondrial cAMP/ PKA signal takes place which causes degradation/proteolysis of Sirt3 that, in turn, promotes hyperacetylation of OPA1 and its proteolytic processing.

2. Materials and methods

2.1. Cell cultures and treatments

The H9c2 cell line, derived from embryonic rat heart, was purchased from American Type Culture Collection (A.T.T.C.#CRL1446, Manassas, VA). Cells were grown in DMEM supplemented with 10% fetal bovine serum (FBS), plus 2 mM glutamine, 100 IU/ml penicillin and 100 IU/ml streptomycin at 37 °C, 10% CO_2.Once at70% confluence, cells were treated with 50 or 100 μM t-BHP. After 45 min of treatment, the medium was changed and the cells cultured for further 2 h, before being used for the analyses. Where indicated 100 μM8-Br-cAMP, 1 μM isoproterenol, 5 μM H89, 100 μM 8-pCPT-2′-O-Me-cAMP (8-(4Chlorophenylthio)-2′-O-methyladenosine3′,5′-cyclic monophosphate monosodium hydrate), 10 μM MG132 or 5 μMepoxomicin were added 30 min before the t-BHP treatments. Further specifications are given in the legends to figures.

2.2. Annexin V and PI binding assay

Annexin V and PI fluorescein staining kit (Invitrogen) was utilized to measure H9c2 cell apoptosis by following the manufacturer's instruction. Briefly, 1×10^6 cells were suspended in 200 μlbinding buffer (10 mM HEPES pH 7.4, 140 mM NaCl, 2.5 mM $CaCl_2$). Cells were then incubated with Annexin V-FITC (1:20) for 3 min followed by incubation with propidium iodide (PI, 1 mg/ml) for 15 min. Apoptosis rate was evaluated by Flow Cytometry (BD FACSCalibur).

2.3. Diamidino-2-phenylinole (DAPI) staining

H9c2 cells were grown onto fibronectin-coated glass-bottom dishes. The living cells were incubated for 5 min with 0.3 μM DAPI, washed with PBS and examined by Laser Scanner Confocal Microscope (LSCM). Images were collected using a 40× objective. The blue fluorescence intensity of DAPI was analyzed by exciting the sample with laser 405 nm. Acquisition, storage, and data analysis were done using Leica software.

2.4. Measurement of mitochondrial membrane potential

The mitochondrial membrane potential in H9c2 cells was measured using LSCM. Images were collected using a 60× objective on cells seeded onto fibronectin-coated glass-bottom dishes. The living cells were incubated for 15 min with 0.3 μM MitoTracker probe (554 nm excitation and 576 nm emission wavelength), washed with Krebs' buffered salt solution (20 mM Hepes, pH 7.4, 135 mM NaCl, 5 mM KCl, 0.4 mM KH_2PO_4, 1 mM MgSO4, 0.1% w/v glucose, 1 mM $CaCl_2$), and examined by LSCM. The red fluorescence intensity of MitoTracker was analyzed by exciting the sample with a solid state laser 552 nm. Acquisition, storage, and data analysis were done using Leica software.

2.5. Electrophoretic procedures and western blotting

The H9c2 cells were harvested from Petri dishes with 0.05% trypsin, 0.02% EDTA, pelleted by centrifugation at 500 ×g and then resuspended and lysed in RIPA buffer containing 150 mM NaCl, 5 mM EDTA, 50 mM Tris/HCl, 0.1% SDS, 1% Triton X-100, pH 7.4, in the presence of a protease inhibitor (0.25 mM PMSF). Proteins from cell lysate, were separated by 8% SDS-polyacrylamide gel electrophoresis (PAGE) and transferred to a nitrocellulose membrane. The membrane was blocked with 5% fatty acid free dry milk in 500 mM NaCl, 20 mM Tris, 0.05% Tween 20 pH 7.4 (TTBS) for 3 h at 4 °C and probed with antibodies against caspase-9 (Thermo scientific, Pierce Antibodies), BAD (Santa Cruz Biotechnology), OPA1 (Thermo scientific, Pierce Antibodies), Sirt3 (Cell signaling), DRP-1 (Santa Cruz Biotechnology), OMA1 (Abcam), cyclophilin F (Abcam), cytochrome c (Cell signaling), acetylated lysine (Cell signaling), ESSS (PRIM) and Tom 20 (Santa Cruz Biotechnology). The control loading was performed with antibody against β-actin (SIGMA). After being washed in TTBS, the membrane was incubated for 60 min with anti-rabbit or anti-mouse IgG peroxidase-conjugate antibody (diluted 1:5000). Immunodetection was then performed, after further TTBS washes, with the enhanced chemiluminescence (ECL) (BioRad, Milan, Italy). Densitometric analysis was performed by VersaDoc imaging system (BioRad, Milan, Italy).

2.6. FRET measurements

H9c2 cells were transfected (transiently) with the EPAC-based FRET sensor target to cytosol (H96) or specifically to mitochondria (4mtH30). After treatments, cells were fixed with 4% paraformaldehyde (PFA) in PBS (pH 7.4) for 20 min at room temperature, then washed three times in PBS and afterwards coverslips were mounted in Mowiol (polyvinyl alcohol 4–88; Sigma-Aldrich, Milan, Italy). Visualization of ECFP-and/or EYFP-expressing cells and detection of FRET was performed on an inverted microscope (Nikon Eclipse TE2000-S) equipped with a monochromator controlled by MetaMorph/MetaFluor software. ECFP was excited at 433 nm and EYFP at 512 nm. Each image was further corrected for ECFP crosstalk and EYFP cross-excitation as shown by Rodighiero et al. [35]. Briefly, images were aligned and corrected for background in the emission windows for FRET (535/30 nm), ECFP (475/30 nm) and acceptor. The obtained netFRET values were analyzed using EYFP (535/26 nm). Each image was further corrected for ECFP MetaMorph and Microsoft Excel software. cross-talk and EYFP cross-excitation. Thus, netFRET = [IFRETbg − ICFPbg × k1 − IYFPbg (K2-αK1)] / (1-K1δ), where IFRETbg, ICFPbg, 2.7. Immunofluorescence and IYFPbg are the background-corrected pixel gray values measured in the FRET, ECFP and EYFP windows, respectively; K1, K2, α Immunocytochemistry was performed as described in [36].Briefly, and δ are calculated to evaluate the crosstalk between donor and cells were grown and treated as described above. The living cells wereincubated with MitoTracker probe (see Section 2.4) and then fixed for 15 min with 4% paraformaldehyde in PBS. Cells were permeabilized with 0.1% Triton X-100 in PBS for 5 min, blocked with 1% PBS-BSA for 30 min, and incubated for 2 h with antibodies specificfor DRP-1
(1:50 dilution) or cytochromes c (1:50 dilution). After washing, cells were incubated with 1:1000 diluted donkey anti-mouse or donkey anti-rabbit antibodies coupled to Alexa-555. The coverslips were mounted on glass slides with Mowiol mounting medium. The fluorescence signals were detected by a confocal microscope Leica.

2.8. Immunoprecipitation

H9c2 cells (0.5 mg protein) were sonicated and 500 μgof protein was incubated at 4 °C in 250 μl of RIPA buffer in the presence of 5 μgof

antibody against OPA1. After 12 h incubation, 50 mg of protein A-sepharose was added to the mixture and the immunocomplex was pelleted by centrifugation and washed with RIPA buffer supplemented with the centrifuged at 2000 × g for 5 min at 4 °C. The supernatant containing the released OPA1 protein was finally collected, separated by SDS-PAGE, transferred to a nitrocellulose membrane and immunoblotted with antibodies against OPA1 and acetyl-lysine.

2.9. Data analysis

All data are presented as means + SEM (standard error of mean). n protease inhibitor cocktail. To separate the protein A-sepharose-antibody complex, the pellet was suspended in 100 mM glycine, pH 2.5 and then

value denotes the number of independent experiments. Statistical difference was determined by Student' t-test. p-Value of 0.05 was considered as statistically significant (**p b 0.01; *p b 0.05).

3. Results

3.1. t-BHP treatment results in a significant accumulation of cellular ROS and induces apoptosis in H9c2 cell cultures

The treatment of H9c2 cell cultures with 50 or 100 μM t-BHP for 45 min resulted, at 2 h by the end of treatment, in a dose dependent increase of the cellular H_2O_2 level, as detected by the redox-sensitive fluorescent probe H2DCFDA (Fig. S1a). Confocal microscopy analysis showed that the t-BHP treatment of H9c2 cell cultures also induced increase in the mitochondrial level of oxygen superoxide detected by the mitoSOX fluorescent probe (Fig. S1b).

Quantitative analysis, using flow cytometry of H9c2 cells stained with Annexin V and PI, showed that the treatment with 50 μM t-BHP significantly increased the number of apoptotic cells (Fig. 1a) comparing to the untreated cells. The treatment with 100 μM t-BHP further increased apoptosis (Fig. 1a). LSCM analysis showed that both concentration of t-BHP increased the DAPI staining of cellular nuclei (Fig. 1b), in agreement with cytofluorimetric analysis. Fig. 1c shows the effects of t-BHP treatments on the mitochondrial membrane potential, monitored by confocal microscopy using the MitoTracker probe. LSCM showed that the treatment of H9c2 cell cultures with 50 or 100 μM t-BHP resulted in a decrease of mitochondrial membrane potential. The images at high magnification show that the mitochondria appeared well networked in untreated cells, and fragmented and punctuated in t-BHP treated cells (Fig. 1c). Immunofluorescence analysis using MitoTracker and cytochrome c antibody showed, as expected, a cytochrome c mitochondrial localization in untreated cells and the release of this protein in the cells treated with 50 and 100 μM t-BHP (Fig. 1d). Immunofluorescence analysis with MitoTracker and DRP-1 antibody showed an increased translocation of DRP-1 into mitochondria in the cells treated with 50 and 100 μMBHP (Fig. 2a).

We next examined the cleavage of caspase-9 and BAD proteins, involved in apoptosis pathway, by western blot analysis with specific antibodies. Decreased levels (proteolysis/activation) of caspase-9 and BAD proteins (Fig. 2b), in t-BHP treated cells were observed with respect to untreated cells. Western blotting analysis with an antibody that recognizes L-OPA1 and S-OPA1 forms revealed that the treatment with t-BHP resulted in appearance of S-OPA1 form (Fig. 2c). No change was observed in OPA1 total protein level (data not shown). Western blotting analysis of Sirt3 showed that the treatment of H9c2 cells, with 50 or 100 μM t-BHP, resulted in a decreased level of this protein (Fig. 2d). All the apoptotic parameters analyzed, were t-BHP dose-dependent (Figs. 1 and 2). Analysis by western blotting of Tom 20 (protein of outer mitochondrial membrane), ESSS (protein of inner membrane) and cyclophilin F (protein of the matrix space) showed that the total mitochondrial protein levels were not affected by t-BHP treatments (Fig. S2).

3.2. FRET analysis of cytosolic and mitochondrial cAMP reveals a selective decrease of mitochondrial cAMP in response to t-BHP treatments

It has been reported that mitochondrial and cytosolic cAMP are involved in apoptosis mechanism [32,37] thus we evaluated their possible changes after t-BHP treatments. Normalized FRET (netFRET) signals in cells transfected with the selective mitochondrial (4mtH30) probe were found to be significantly higher at 5 and 10 min of treatment with 50 μM(Fig. 3a) or 100 μM(Fig. 3b) t-BHP and restored at 45 min. Based on FRET probe features, these observations are consistent with a significant decrease of the mitochondrial level of cAMP upon t-BHP treatments. No changes in FRET signals were measured in cells transfected with the FRET probe to detect cytosolic cAMP (Fig. 3a, b).

3.3. 8-Br-cAMP prevents apoptosis in H9c2 cell cultures

Based on these results, we have tested the effect of pretreatment (30 min) of H9c2 cell cultures with β-agonist isoproterenol or 8bromoadenosine 3′,5′-cyclic monophosphate (8-Br-cAMP) on apoptosis induced by t-BHP. Interestingly, confocal analysis showed that the bright DAPI staining of the cells treated with 50 or 100 μM t-BHP was prevented by 8-Br-cAMP, but not by isoproterenol (Fig. 4a). The prevention effect exerted by 8-Br-cAMP was observed also in cytofluorimetric anexin + PI test (Fig. 4b) and mitochondrial membrane potential analysis (Fig. 4c). Furthermore the pretreatment with 8-Br-cAMP prevents the appearance of fragmented mitochondria in t-BHP treated cells (Fig. 4c). Western blotting analysis with antibodies against caspase-9 and BAD proteins showed that 8-Br-cAMP, but not isoproterenol, prevented the t-BHP-induced decrease of these proteins (Fig. 4d), confirming the prevention of apoptosis by 8-Br-cAMP. As shown in Fig. 5 the pretreatment with 8-Br-cAMP also prevented the appearance of S-OPA1 form (Fig. 5a) and the decrease of Sirt3 protein level (Fig. 5b)in t-BHP treated cells. No effect was observed in the presence of isopro-conditions (Fig. S3). The effects of 8-Br-cAMP and isoproterenol have terenol (Fig. 5a). OMA1 is involved in proteolytic processing of OPA1 been analyzed on H9c2 control cells (untreated). Western blotting analand its degradation/activation has been reported in stress condition, yses showed that the total mitochondrial proteins (Tom 20, ESSS and thus we examined the protein level of OMA1. Western blotting analysis cyclophilin F proteins) (Fig. S2), caspase-9, BAD, OPA1 and Sirt3 (Fig. showed that no change in OMA1 level was present in our experimental S4) were not affected by these treatments.

3.4. cAMP/PKA pathway and mitochondrial proteases are involved in the prevention of apoptosis

cAMP cascade can have, as targets, PKA or exchange protein directly activated by cAMP (Epac). The downstream targets of cAMP involved in the prevention of apoptosis were evaluated using H89, inhibitor of PKA and 8-pCPT-2′-O-Me-cAMP (8pCPT), analog of cAMP specific for Epac activation. Fig. 6 shows that H89 abolished the positive effect exerted by 8-Br-cAMP on apoptosis as show by DAPI staining (Fig. 6a). No change in nuclei DAPI staining after t-BHP treatment was observed in 8pCPT pretreated cells (Fig. 6a). Furthermore the data presented in Fig. 6b show that the pretreatment of the H9c2 cells with MG132, an inhibitor of proteasome, as well as, of mitochondrial Lon proteases [38,39], prevented the t-BHP-induced apoptosis (Fig. 6b) while the pretreatment with epoxomicin, a specific proteasome inhibitor [40] had no effect (Fig. 6b). Moreover, MG132 also prevented apoptosis in the presence of 8-Br-cAMP plus H89 (Fig. 6b). Fig. 6c shows the effects of 8-Br-cAMP, H89, 8pCPT, MG132, epoxomicin and their combination on decreased level (proteolysis/activation) of caspase-9 in the t-BHP treated cells. The H89 abolished the positive effect exerted by 8-Br-cAMP on the t-BHP-dependent decrease of caspase-9. No effect was observed in the cells pretreated with 8pCPT or epoxomicin. Again, the pretreatment of the H9c2 cells with MG132, alone or in the presence of 8-Br-cAMP and H89, prevented the t-BHP-dependent decrease of caspase-9 (Fig. 6c).

As shown by LSCM images, the t-BHP-dependent decrease of membrane potential and the t-BHP-dependent mitochondrial fragmentation (Fig. 7), as well as, the cytochrome c release (Fig. S5) were prevented by 8-Br-cAMP. H89 removed the positive effect exerted by 8-Br-cAMP. The cells pretreatment with 8pCPT or epoxomicin did not prevent these mitochondrial parameters. MG132 alone or in combination with 8-BrcAMP and H89 prevented the t-BHP-dependent decrease of mitochondrial membrane potential and t-BHP-dependent mitochondrial fragmentation (Fig. 7) and the cytochrome c release (Fig. S5).

Immunofluorescence analysis of DRP-1 localization showed that the pretreatment of the cells with 8-Br-cAMP prevented the t-BHP-induced mitochondrial translocation (Fig. 8). The presence of H89 abolished the effect of 8-Br-cAMP. The analysis of the pretreated cells with 8pCPT showed a partially mitochondrial translocation and much cellular diffusion of DRP-1. In the pretreated cells with epoxomicin or MG132, alone or in combination with 8-Br-cAMP and H89, DRP-1 appeared to be almost totally co-localizated with mitochondria with low cellular diffusion (Fig. 8).

We next examined the effects of 8-Br-cAMP, H89, 8pCPT, MG132, epoxomicin and their combination on Sirt3 protein level. The treatment of H9c2 cell cultures with H89 abrogated the positive effect of 8-Br-cAMP on Sirt3 protein level (Fig. 9a), 8pCPT and epoxomicin did not avoid the decrease of Sirt3 protein level in t-BHP treated cells. MG132 alone, or in combination with 8-Br-cAMP and H89, prevented the t-BHP-induced decrease of Sirt3 (Fig. 9a). No effects were observed on Sirt3 and caspase-9 protein levels and mitochondrial membrane potential and network, when 8-Br-cAMP, H89, 8pCPT, MG132, epoxomicin were used on untreated cells (Fig. S6). Fig. 9b shows the acetylation status of OPA1. The OPA1 was immunoprecipitated from untreated cells, t-BHP-treated cells and pretreated cells with 8-Br-cAMP or MG132. The western blotting analysis on the immuno-precipitated samples, performed with antibody against acetylated lysine, showed bands at the same molecular weight of those immuno-revealed by the antibody against OPA1 (Fig. 9b). In the t-BHP treated cells the antibody against acetyl-lysine also immuno-revealed bands corresponding to the S-OPA1 forms that were only partially detectable in 8-Br-cAMP or MG132 preatreated cells (Fig. 9b). The densitometric analysis shows that the acetylation bands, normalized on the amount of immuno-precipitated OPA1, resulted more abundant in t-BHP treated cells with respect to untreated cells (Fig. 9b). The pretreatment with 8-Br-cAMP or MG132 reduced the increase of acetylation (Fig. 9b).

4. Discussion

Cardiac diseases are associated with increased ROS level and mitochondrial dysfunction that bring to mitochondrial apoptosis [4,41]. Although, the molecular mechanism of mitochondrial apoptosis is largely studied, the molecular components regulating mitochondrial network remain to be completed and interconnected among them. In fact, a number of signals and proteins have been found to be involved in this process. Among these, cAMP signal, OPA1 fusion protein and Sirt3 deacetylase enzyme represent an example of signals and proteins that govern the mitochondrial metabolism and that are involved in the mitochondrial apoptosis. The present work shows a possible mechanism networking these main actors in cardiomyoblasts H9c2 cells.

The oxidative stress triggers a series of events which lead to apoptosis of these cells, as shown by caspase proteolysis/activation, cytochrome c release, DRP-1 translocation, changes in the mitochondrial morphology, appearance of S-OPA1 form and reduction of mitochondrial Sirt3 protein level (Figs. 1 and 2). The analysis of cAMP levels, by FRET, shows a selective and rapid loss of mitochondrial cAMP which seems to play an important role in triggering apoptosis, no effect has been observed in the cytosolic cAMP level. Indeed, all the analyzed parameters of mitochondrial apoptotic pathway indicate that the pretreatment of the cells with the permeable analogous of cAMP, 8-Br-cAMP, prevents the triggering of events that lead to apoptosis. Interestingly pretreatment with β-agonist, isoproterenol, that induces activation of tmAC with increasing of cytosolic cAMP, had no effect in preventing apoptosis, indicating a specificroleof mitochondrial pool of cAMP in the prevention of apoptosis in H9c2 cells. Several studies report mitochondrial activation of mitochondrial proteases [29]. Insight into the mechanism of the role of mitochondrial cAMP in the t-BHP-induced apoptosis is provided by the effect of the protease inhibitors on the Sirt3 protein level. In fact, MG132, an inhibitor of mitochondrial proteases as well as of the cytosolic proteasome [see refs. 38, 39] rescued the protein level of Sirt3 and the tBHP-induced apoptosis in H9c2 cells. Epoxomicin, that inhibits specifically the cytosolic proteasome had no effect in these conditions. This indicates a role of mitochondrial proteases in t-BHP-induced apoptosis. Furthermore, MG132 prevented apoptosis also in the presence of H89 that, in turn, abolished the effect of 8-Br-cAMP on t-BHP-induced apoptosis, suggesting a downstream effect of MG132.MG132 pretreatment,as well as 8-Br-cAMP, also rescued the t-BHP-induced mitochondrial fragmentation. The fragmentation occurring during the apoptotic stress appears to be associated with both OPA1 degradation and DRP-1 mitochondrial translocation (Figs. 1 and 2). The prevention effect 8-BrcAMP was exerted on both OPA1 digestion and DRP-1 mitochondrial translocation (Figs. 5 and 8), in fact 8-Br-cAMP is a permeant analog of cAMP that, acting widely, can activate the cytosolic PKA that, in turn, phosphorylates DRP-1 inhibiting its mitochondrial translocation [51]. However, the activation of cytosolic cAMP cascade by isoproterenol did not prevent stress-induced apoptosis, as showed by DAPI staining and cytofluorimetric analysis (Fig. 4), and OPA1 processing (Fig. 5). Moreover, MG132, that prevented apoptosis (Fig. 6) and OPA1 processing (Fig. 9) did not prevent the t-BHP-induced DRP1 mitochondrial translocation. All these data suggest that the change of mitochondrial morphology is due mainly to OPA1. Furthermore, it has been observed an increase of the acetylation status of OPA1 in the t-BHP treated cells that was prevented by both 8-Br-cAMP and MG132 (Fig. 9). However, even if the OPA1 processing is prevented by MG132, its acetylation status, although reduced with respect to t-BHP-treated cells, according to the increased Sirt3 level, appears to be abundant indicating that another additional mechanism could take place in the presence of MG132.

Thus, our data indicate that the reduction of mitochondrial cAMP pool morphology changes during apoptosis with the involvement of DRP-1 and OPA1 [13,42],in particular OPA1 mitochondrial fusion protein is involved in these morphological changes during heart failure [14], and overexpression of OPA1 confers apoptotic resistance [43], whereas loss OPA1 increases the apoptotic sensitivity of cells [44]. In addition, apoptosis is associated to complete conversion of L-OPA1 in S-OPA1. The present results show that decrease of mitochondrial cAMP level is associated with the appearance of S-OPA1 form which was prevented by 8-Br-cAMP, but not by isoproterenol. cAMP has as targets PKA and Epac, both found to be localized in the mitochondria [45–47]. The data show that the positive effect in the prevention of apoptosis exerted by 8-Br-cAMP was abolished by H89, inhibitor of PKA, while Epac activation by 8-pCPT-2′-O-Me-cAMP had no effect in the prevention of apoptosis, thus indicating an involvement of cAMP/PKA pathway. Our results demonstrate that the level of mitochondrial cAMP can control the processing of OPA1. In addition OPA1 is hyperacetylated under stress conditions and Sirt3 deacetylates and activates OPA1 [48]. The mitochondrial deacetylase Sirt3, regulates the activity of numerous mitochondrial enzymes, is portrayed as a mitochondrial fidelity protein [49]. We found that t-BHP treatment and apoptosis are associated with a decreased level of Sirt3. A previous work [50] observed that exogenous cAMP increased Sirt3 level and speculated about a possible susceptibly of Sirt3 for mitochondrial proteases under reduction of cAMP level. Furthermore, we showed that a decrease of mitochondrial cAMP resulted in an

Fig. 8. Effect of cAMP/PKA signaling and MG132 on DRP-1 mitochondrial translocation. For experimental conditions see the legend to Fig. 6. Representative images by LSCM of immunofluorescence of H9c2 cells probed with MitoTracker and immunostained with antibody against DRP-1.

lead to reduction of Sirt3 protein level by its degradation that, in turn, causes a hyperacetylation of OPA1 [48]. This triggers the conversion of L.-OPA1 into S-OPA1 and consequent mitochondrial apoptosis. The sustained level of cAMP, by a preventive addition to H9c2 cell cultures of 8-Br-cAMP, reduces the number of cells undergoing apoptosis promoting cell life. In conclusion this study correlates the two main post-translational modifications, phosphorylation and acetylation, that regulate the mitochondrial activities.

Conflict of interest

The authors declare that they have no conflict of interest.

Transparency document

The Transparency document associated with this article can be found, in online version.

Acknowledgments

This work has been supported by a grant to D.D.R. from MIUR (Progetto FIRB futuro in ricerca, 2008) [RBFR0813Z5]. We thank Dr. Giulietta Di Benedetto for providing the matrix-targeted cAMP sensor 4mtH30 and for critical reading of the manuscript.

Appendix A. Supplementary data

Supplementary data to this article can be found online at http://dx.doi.org/10.1016/j.bbamcr.2016.11.022.

References

[1] D. Bryant, L. Becker, J. Richardson, J. Shelton, F. Franco, R. Peshock, M. Thompson, B. Giroir, Cardiac failure in transgenic mice with myocardial expression of tumor necrosis factor-alpha, Circulation 97 (1998) 1375–1381.

[2] J. Wang,J.P.Silva,C.M.Gustafsson, P. Rustin, N.G.Larsson,Increased in vivo apoptosisin cells lacking mitochondrial DNA gene expression, Proc. Natl. Acad. Sci. U. S. A. 98 (7) (2001) 4038–4043.

[3] M.R. Sayen, A.B. Gustafsson, M.A. Sussman, J.D. Molkentin, R.A. Gottlieb, Calcineurin transgenic mice have mitochondrial dysfunction and elevated superoxide production, Am. J. Phys. Cell Phys. 284 (2) (2003) C562–C570.

[4] A.B. Gustafsson, R.A. Gottlieb, Heart mitochondria: gates of life and death, Cardiovasc. Res. 77 (2) (2008) 334–343.

[5] S. Papa, D. De Rasmo, S. Scacco, A. Signorile, Z. Technikova-Dobrova, G. Palmisano, A.M. Sardanelli, F. Papa, D. Panelli, R. Scaringi, A. Santeramo, Mammalian complex I: a regulable and vulnerable pacemaker in mitochondrial respiratory function, Biochim. Biophys. Acta 1777 (7–8) (2008) 719–728, http://dx.doi.org/10.1016/j.bbabio.2008.04.005.

[6] D. DeRasmo,A.Signorile, M. Larizza,C.Pacelli, T. Cocco,S.Papa, Activation of the cAMP cascade in human fibroblast cultures rescues the activity of oxidatively damaged complex I, Free Radic. Biol. Med. 52 (4) (2012) 757–764, http://dx.doi.org/10.1016/j.freeradbiomed.2011.11.030.

[7] H. Tsutsui, S. Kinugawa, S. Matsushima, Mitochondrial oxidative stress and dysfunction in myocardial remodelling, Cardiovasc. Res. 81 (3) (2009) 449–456, http://dx.doi.org/10.1093/cvr/cvn280.

fragmentation cause heart failure in mice, Science 350 (6265) (2015), aad0116 http://dx.doi.org/10.1126/science.aad0116 (4).

[17] T.K. Rainbolt, J. Lebeau, C. Puchades, Wiseman RL (2016) reciprocal degradation of YME1L and OMA1 adapts mitochondrial proteolytic activity during stress, Cell Rep. 14 (9) (Mar 8 2016) 2041–2049, http://dx.doi.org/10.1016/j.celrep.2016.02.011.

[18] C.J. Chen, Y.C. Fu, W. Yu, W. Wang, SIRT3 protects cardiomyocytes from oxidative stress-mediated cell death by activating NF-κB, Biochem. Biophys. Res. Commun. 430 (2) (2013) 798–803, http://dx.doi.org/10.1016/j.bbrc.2012.11.066.

[19] T.Y. Alhazzazi, P. Kamarajan, E. Verdin, Y.L. Kapila, SIRT3 and cancer: tumor promoter or suppressor? Biochim. Biophys. Acta 1816 (1) (2011) 80–88, http://dx.doi.org/10.1016/j.bbcan.2011.04.004.

[20] B. Kincaid, E. Bossy-Wetzel, Forever young: SIRT3 a shield against mitochondrial meltdown, aging, and neurodegeneration, Front. Aging Neurosci. 6 (2013) 5–48, http://dx.doi.org/10.3389/fnagi.2013.00048.

[21] R.K. Perera, V.O. Nikolaev, Compartmentation of cAMP signalling in cardiomyocytes in health and disease, Acta Physiol (Oxford) 207 (4) (2013) 650–662, http://dx.doi.org/10.1111/apha.12077.

[22] D. De Rasmo, A. Signorile, F. Papa, E. Roca, S. Papa, cAMP/Ca2+ response elementbinding protein plays a central role in the biogenesis of respiratory chain proteins in mammalian cells, IUBMB Life 62 (6) (2010) 447–452, http://dx.doi.org/10. 1002/iub.342.

[23] G. Di Benedetto, E. Scalzotto, M. Mongillo, T. Pozzan, Mitochondrial Ca^{2+} uptake induces cyclic AMP generation in the matrix and modulates organelle ATP levels, Cell Metab. 17 (6) (2013) 965–975, http://dx.doi.org/10.1016/j.cmet.2013.05.003.

[24] F. Valsecchi, L.S. Ramos-Espiritu, J. Buck, L.R. Levin, G. Manfredi, cAMP and mitochondria, Physiology (Bethesda) 28 (3) (2013) 199–209, http://dx.doi.org/10.1152/physiol.00004.2013.

[25] J.H. Zippin, Y. Chen, P. Nahirney, M. Kamenetsky, M.S. Wuttke, D.A. Fischman, L.R. Levin, J. Buck, Compartmentalization of bicarbonate-sensitive adenylyl cyclase in distinct signaling microdomains, FASEB J. 17 (1) (2003) 82–84.

[26] D. De Rasmo, G. Gattoni, F. Papa, A. Santeramo, C. Pacelli, T. Cocco, L. Micelli, N. Sardaro, M. Larizza, M. Scivetti, S. Milano, A. Signorile, The β-adrenoceptor agonist isoproterenol promotes the activity of respiratory chain complex I and lowers cellular reactive oxygen species in fibroblasts and heart myoblasts, Eur. J. Pharmacol. 652 (1–3) (2011) 15–22, http://dx.doi.org/10.1016/j.ejphar.2010.11.016.

[27] R. Acin-Perez, E. Salazar, S. Brosel, H. Yang, E.A. Schon, G. Manfredi, Modulation of mitochondrial protein phosphorylation by soluble adenylyl cyclase ameliorates cytochrome oxidase defects, EMBO Mol. Med. 1 (8–9) (2009) 392–406, http://dx.doi.org/10.1002/emmm.200900046.

[28] D. De Rasmo, A. Signorile, A. Santeramo, M. Larizza, P. Lattanzio, G. Capitanio, S. Papa, Intramitochondrial adenylyl cyclase controls the turnover of nuclear-encoded subunits and activity of mammalian complex I of the respiratory chain, Biochim. Biophys. Acta 1853 (1) (2015) 183–191, http://dx.doi.org/10.1016/j.bbamcr.2014.10.016.

[29] D. De Rasmo, L. Micelli, A. Santeramo, A. Signorile, P. Lattanzio, S. Papa, cAMP regulates the functional activity, coupling efficiency and structural organization of mammalian FOF1 ATP synthase, Biochim. Biophys. Acta 1857 (4) (2016) 350–358, http://dx.doi.org/10.1016/j.bbabio.2016.01.006.

[30] E. Iwai-Kanai, K. Hasegawa, M. Araki, T. Kakita, T. Morimoto, S. Sasayama, Alpha and beta-adrenergic pathways differentially regulate cell type-specific apoptosis in rat cardiac myocytes, Circulation 100 (1999) 305–311.

[31] C. Krakstad, A.E. Christensen, S.O. Doskeland, cAMP protects neutrophils against TNF-alpha-induced apoptosis by activation of cAMP-dependent protein kinase, independently of exchange protein directly activated by cAMP (Epac), J. Leukoc. Biol. 76 (2004) 641–647.

[32] A.F. Branco, S.F. Sampaio, M.R. Wieckowski, V.A. Sardão, P.J. Oliveira, Mitochondrial disruption occurs downstream from β-adrenergic overactivation by isoproterenol in differentiated, but not undifferentiated H9c2 cardiomyoblasts: differential activation of stress and survival pathways, Int. J. Biochem. Cell Biol. 45 (11) (2013) 2379–2391, http://dx.doi.org/10.1016/j.biocel.2013.08.006.

[8] A. Olichon, L. Baricault, N. Gas, E. Guillou, A. Valette, P. Belenguer, G. Lenaers, Loss of OPA1 perturbates the mitochondrial inner membrane structure and integrity, leading to cytochrome c release and apoptosis, J. Biol. Chem. 278 (10) (2003) 7743–7746.

[9] G. Twig, A. Elorza, A.J. Molina, H. Mohamed, J.D. Wikstrom, G. Walzer, L. Stiles, S.E. Haigh, S. Katz, G. Las, J. Alroy, M. Wu, B.F. Py, J. Yuan, J.T. Deeney, B.E. Corkey, O.S. Shirihai, Fission and selective fusion govern mitochondrial segregation and elimination by autophagy, EMBO J. 27 (2) (2008) 433–446, http://dx.doi.org/10.1038/sj. emboj.7601963.

[10] V.B. Pillai, N.R. Sundaresan, V. Jeevanandam, M.P. Gupta, Mitochondrial SIRT3 and heart disease, Cardiovasc. Res. 88 (2) (2010) 250–256, http://dx.doi.org/10.1093/ cvr/cvq250.

[11] Y. Ladilov, A. Appukuttan, Role of soluble adenylyl cyclase in cell death and growth, Biochim. Biophys. Acta 1842 (2014) 2646–2655, http://dx.doi.org/10.1016/j.bbadis.2014.06.034.

[12] B. Ugarte-Uribe, A.J. García-Sáez, Membranes in motion: mitochondrial dynamics and their role in apoptosis, Biol. Chem. 395 (3) (2014) 297–311, http://dx.doi.org/10.1515/hsz-2013-0234.

[13] A. Alaimo, R.M. Gorojod, J. Beauquis, M.J. Muñoz, F. Saravia, M.L. Kotler, Deregulation of mitochondria-shaping proteins Opa-1 and Drp-1 in manganese-induced apoptosis, PLoS One 9 (3) (2014), e91848 http://dx.doi.org/10.1371/journal.pone.0091848 (14).

[14] L. Chen, Q. Gong, J.P. Stice, A.A. Knowlton, Mitochondrial OPA1, apoptosis, and heart failure, Cardiovasc. Res. 84 (1) (2009) 91–99, http://dx.doi.org/10.1093/cvr/cvp181.

[15] R. Anand, T. Wai, M.J. Baker, N. Kladt, A.C. Schauss, E. Rugarli, T. Langer, The i-AAA protease YME1L and OMA1 cleave OPA1 to balance mitochondrial fusion and fission, J. Cell Biol. 204 (6) (2014) 919–929, http://dx.doi.org/10.1083/jcb.201308006.

[16] T. Wai, J. García-Prieto, M.J. Baker, C. Merkwirth, P. Benit, P. Rustin, F.J. Rupérez, C. Barbas, B. Ibañez, T. Langer, Imbalanced OPA1 processing and mitochondrial

[33] R. Palorini, D. De Rasmo, M. Gaviraghi, L. Sala Danna, A. Signorile, C. Cirulli, F. Chiaradonna, L. Alberghina, S. Papa, Oncogenic K-ras expression is associated with derangement of the cAMP/PKA pathway and forskolin-reversible alterations of mitochondrial dynamics and respiration, Oncogene 32 (3) (2013) 352–362.

[34] J. Hescheler, R. Meyer, S. Plant, D. Krautwurst, W. Rosenthal, G. Schultz, Morphological, biochemical, and electrophysiological characterization of a clonal cell (H9c2) line from rat heart, Circ. Res. 69 (1991) 1476–1486.

[35] S. Rodighiero, C. Bazzini, M. Ritter, J. Furst, G. Botta, G. Meyer, M. Paulmichl, Fixation, mounting and sealing with nail polish of cell specimens lead to incorrect FRET measurements using acceptor photobleaching, Cell. Physiol. Biochem. 21 (5–6) (2008) 489–498, http://dx.doi.org/10.1159/000129642.

[36] A. Iolascon, V. Aglio, G. Tamma, M. D'Apolito, F. Addabbo, G. Procino, M.C. Simonetti, G. Montini, L. Gesualdo, E.W. Debler, M. Svelto, G. Valenti, Characterization of two novel missense mutations in the AQP2 gene causing nephrogenic diabetes insipidus, Nephron Physiol. 105 (3) (2007) 33–41.

[37] S. Kumar, S. Kostin, J.P. Flacke, H.P. Reusch, Y. Ladilov, Soluble adenylyl cyclase controls mitochondria-dependent apoptosis in coronary endothelial cells, J. Biol. Chem. 284 (22) (2009) 14760–14768, http://dx.doi.org/10.1074/jbc.M900925200.

[38] V. Azzu, M.D. Brand, Degradation of an intramitochondrial protein by the cytosolic proteasome, J. Cell Sci. 123 (2010) 578–585, http://dx.doi.org/10.1242/jcs.060004.

[39] Z. Granot, O. Kobiler, N. Melamed-Book, S. Eimerl, A. Bahat, B. Lu, S. Braun, M.R. Maurizi, C.K. Suzuki, A.B. Oppenheim, J. Orly, Turnover of mitochondrial steroidogenic acute regulatory (StAR) protein by Lon protease: the unexpected effect of proteasome inhibitors, Mol. Endocrinol. 21 (2007) 2164–2177.

[40] L. Meng, R. Mohan, B.H. Kwok, M. Elofsson, N. Sin, C.M. Crews, Epoxomicin, a potent and selective proteasome inhibitor, exhibits in vivo antiinflammatory activity, Proc. Natl. Acad. Sci. U. S. A. 96 (1999) 10403–10408.

[41] Y. Lee, A.B. Gustafsson, Role of apoptosis in cardiovascular disease, Apoptosis 14 (4) (2009) 536–548, http://dx.doi.org/10.1007/s10495-008-0302-x.

[42] S. Frank, B. Gaume, E.S. Bergmann-Leitner, W.W. Leitner, E.G. Robert, F. Catez, C.L. Smith, R.J. Youle, The role of dynamin-related protein 1, a mediator of mitochondrial fission, in apoptosis, Dev. Cell 1 (4) (2001) 515–525.

[43] C. Frezza, S. Cipolat, O. Martins de Brito, M. Micaroni, G.V. Beznoussenko, T. Rudka, D. Bartoli, R.S. Polishuck, N.N. Danial, B. De Strooper, L. Scorrano, OPA1 controls apoptotic cristae remodeling independently from mitochondrial fusion, Cell 126 (1) (2006) 177–189.

[44] S. Cipolat, T. Rudka, D. Hartmann, V. Costa, L. Serneels, K. Craessaerts, K. Metzger, C. Frezza, W. Annaert, L. D'Adamio, C. Derks, T. Dejaegere, L. Pellegrini, R. D'Hooge, L. Scorrano, B. De Strooper, Mitochondrial rhomboid PARL regulates cytochrome c release during apoptosis via OPA1-dependent cristae remodeling, Cell 126 (1) (2006) 163–175.

[45] J. Qiao, F.C. Mei, V.L. Popov, L.A. Vergara, X. Cheng, Cell cycle-dependent subcellular localization of exchange factor directly activated by cAMP, J. Biol. Chem. 277 (29) (2002) 26581–26586.

[46] A.M. Sardanelli, A. Signorile, R. Nuzzi, D. De Rasmo, Z. Technikova-Dobrova, Z. Drahota, A. Occhiello, A. Pica, S. Papa, Occurrence of A-kinase anchor protein and associated cAMP-dependent protein kinase in the inner compartment of mammalian mitochondria, FEBS Lett. 580 (24) (2006) 5690–5696.

[47] K. Lefkimmiatis, D. Leronni, A.M. Hofer, The inner and outer compartments of mitochondria are sites of distinct cAMP/PKA signaling dynamics, J. Cell Biol. 202 (3) (2013) 453–462, http://dx.doi.org/10.1083/jcb.201303159.

[48] S.A. Samant, H.J. Zhang, Z. Hong, V.B. Pillai, N.R. Sundaresan, D. Wolfgeher, S.L. Archer, D.C. Chan, M.P. Gupta, SIRT3 deacetylates and activates OPA1 to regulate mitochondrial dynamics during stress, Mol. Cell. Biol. 34 (5) (2014) 807–819, http://dx.doi.org/10.1128/MCB.01483-13.

[49] E.L. Bell, L. Guarente, The SirT3 divining rod points to oxidative stress, Mol. Cell 42 (2011) 561–568, http://dx.doi.org/10.1016/j.molcel.2011.05.008.

[50] Z. Wang, L. Zhang, Y. Liang, C. Zhang, Z. Xu, L. Zhang, R. Fuji, W. Mu, L. Li, J. Jiang, Y. Ju, Z. Wang, Cyclic AMP mimics the anti-ageing effects of calorie restriction by up-regulating sirtuin, Sci. Rep. 5 (2015) 12012, http://dx.doi.org/10.1038/srep12012.

[51] L.C. Gomes, G. Di Benedetto, L. Scorrano, During autophagy mitochondria elongate, are

spared from degradation and sustain cell viability, Nat. Cell Biol. 13 (5) (2011) 589–598, http://dx.doi.org/10.1038/ncb2220.

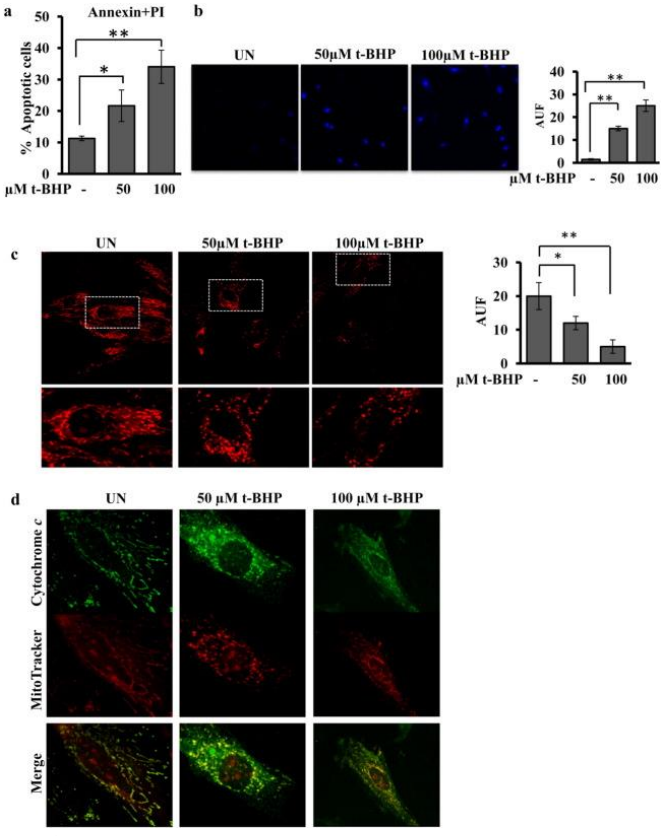

Fig1

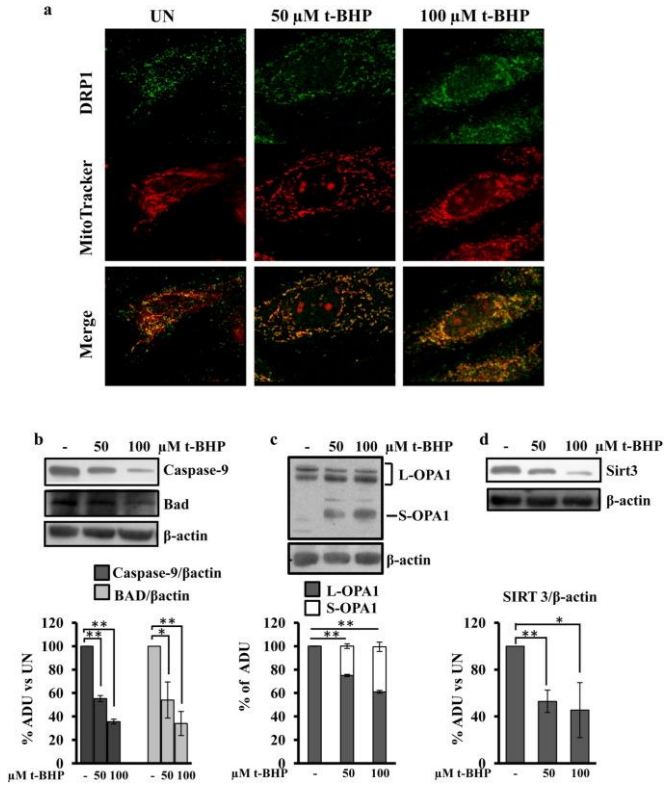
a
UN
50 µM t-BHP
100 µM t-BHP
DRP1
MitoTracker
Merge
b
- 50 100 µM t-BHP
Caspase-9
Bad
β-actin
Caspase-9/βactin
BAD/βactin
% ADU vs UN
µM t-BHP
c
- 50 100 µM t-BHP
L-OPA1
S-OPA1
β-actin
L-OPA1
S-OPA1
% of ADU
µM t-BHP
d
- 50 100 µM t-BHP
Sirt3
β-actin
SIRT 3/β-actin
% ADU vs UN
µM t-BHP

Fig.2

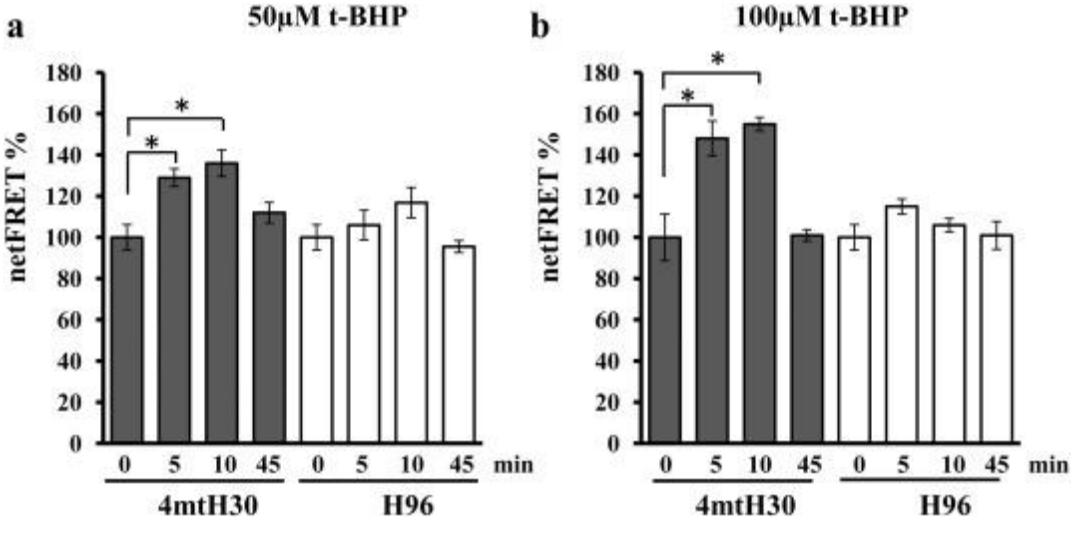
a
50µM t-BHP
netFRET %
0 5 10 45 0 5 10 45 min
4mtH30
H96
b
100µM t-BHP
netFRET %
0 5 10 45 0 5 10 45 min
4mtH30
H96

Fig.3

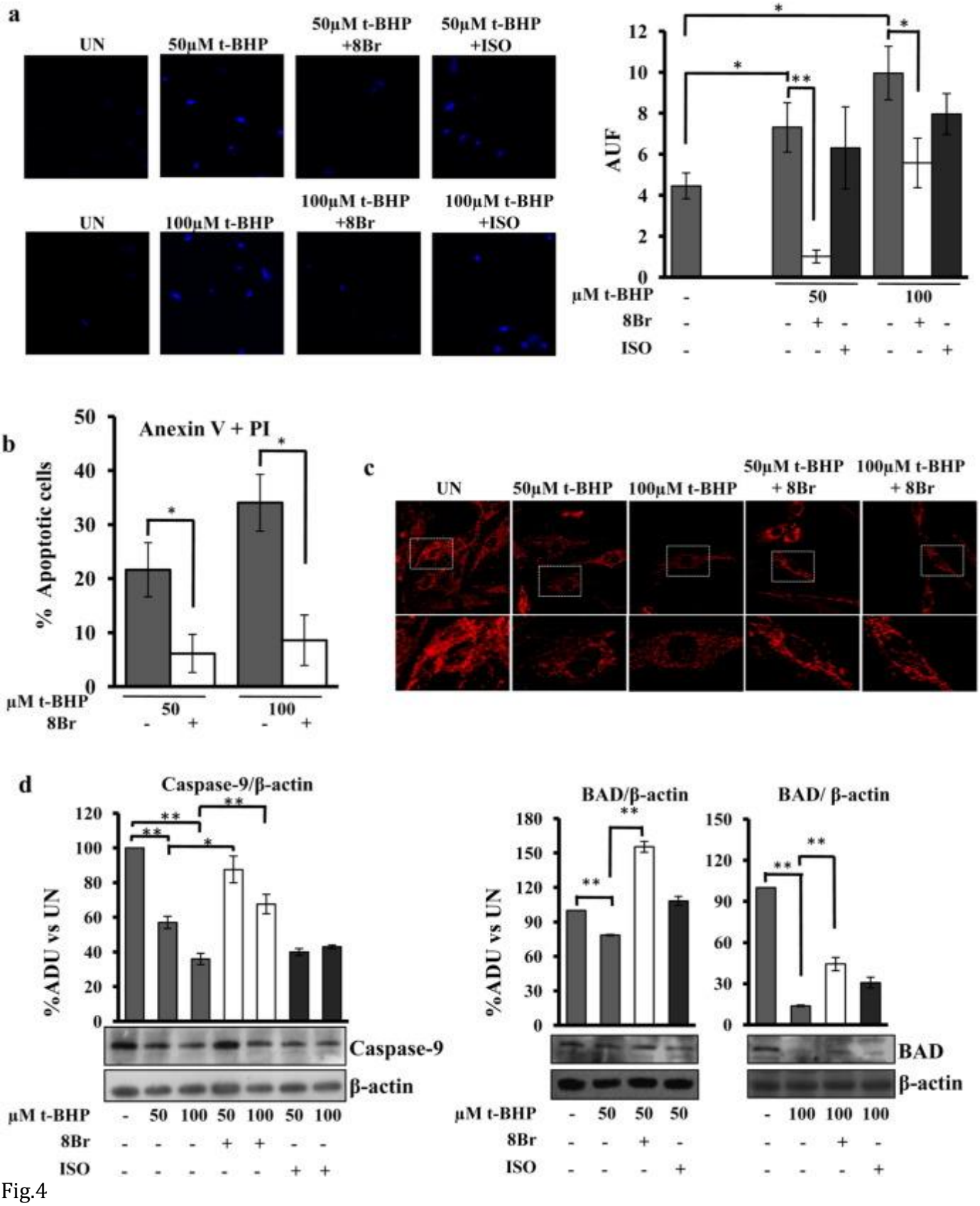
a
UN
50μM t-BHP
50μM t-BHP +8Br
50μM t-BHP +ISO
UN
100μM t-BHP
100μM t-BHP +8Br
100μM t-BHP +ISO
AUF
μM t-BHP
8Br
ISO
b
Anexin V + PI
% Apoptotic cells
μM t-BHP
8Br
c
UN
50μM t-BHP
100μM t-BHP
50μM t-BHP + 8Br
100μM t-BHP + 8Br
d
Caspase-9/β-actin
%ADU vs UN
Caspase-9
β-actin
μM t-BHP
8Br
ISO
BAD/β-actin
BAD/ β-actin
%ADU vs UN
BAD
β-actin
μM t-BHP
8Br
ISO

Fig.4

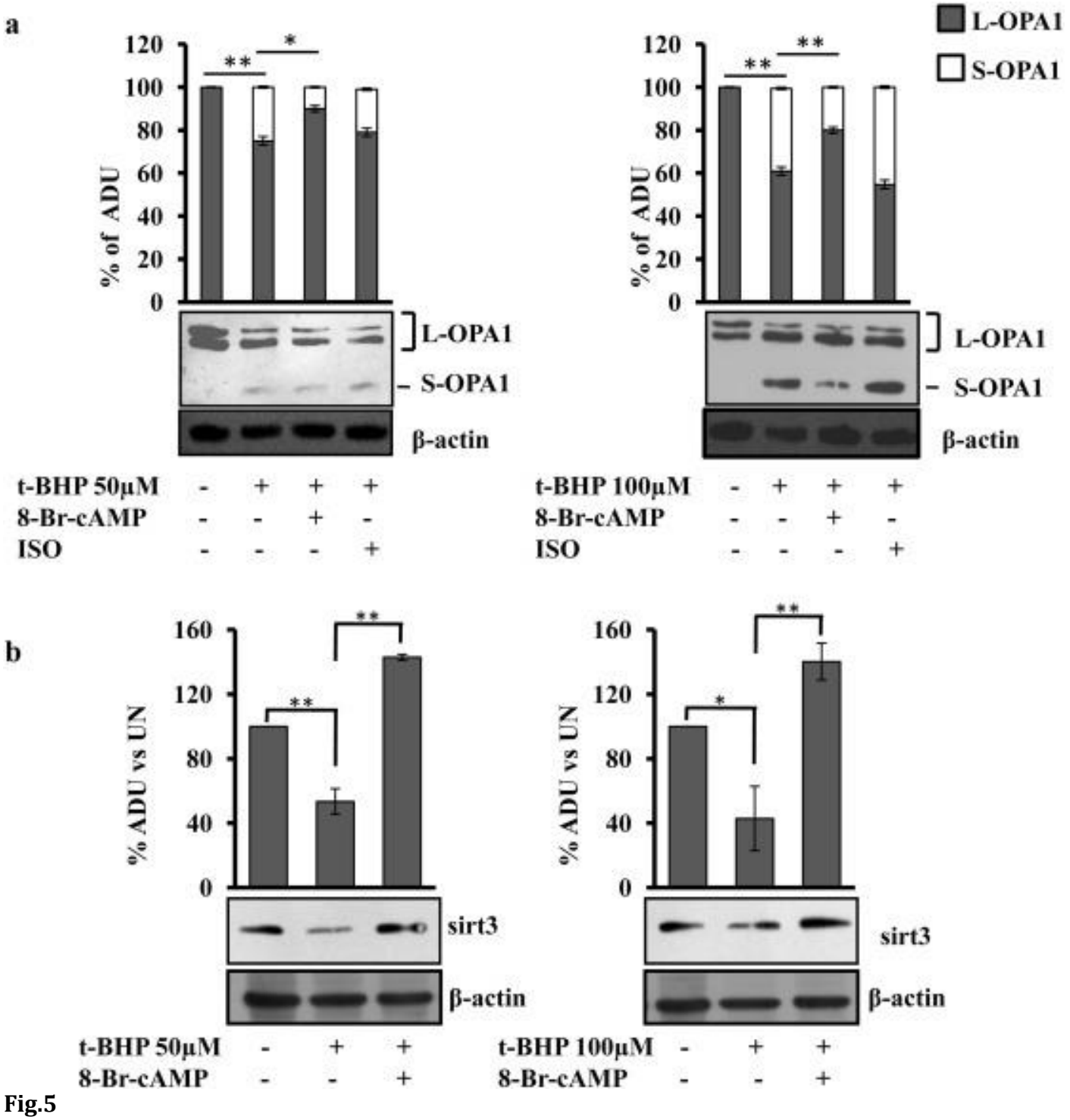
a
L-OPA1
S-OPA1
% of ADU
120
100
80
60
40
20
0
**
*
**
**
L-OPA1
S-OPA1
β-actin
t-BHP 50μM - + + +
8-Br-cAMP - - + -
ISO - - - +
t-BHP 100μM - + + +
8-Br-cAMP - - + -
ISO - - - +
b
% ADU vs UN
160
120
80
40
0
**
**
*
**
sirt3
β-actin
t-BHP 50μM - + +
8-Br-cAMP - - +
t-BHP 100μM - + +
8-Br-cAMP - - +

Fig.5

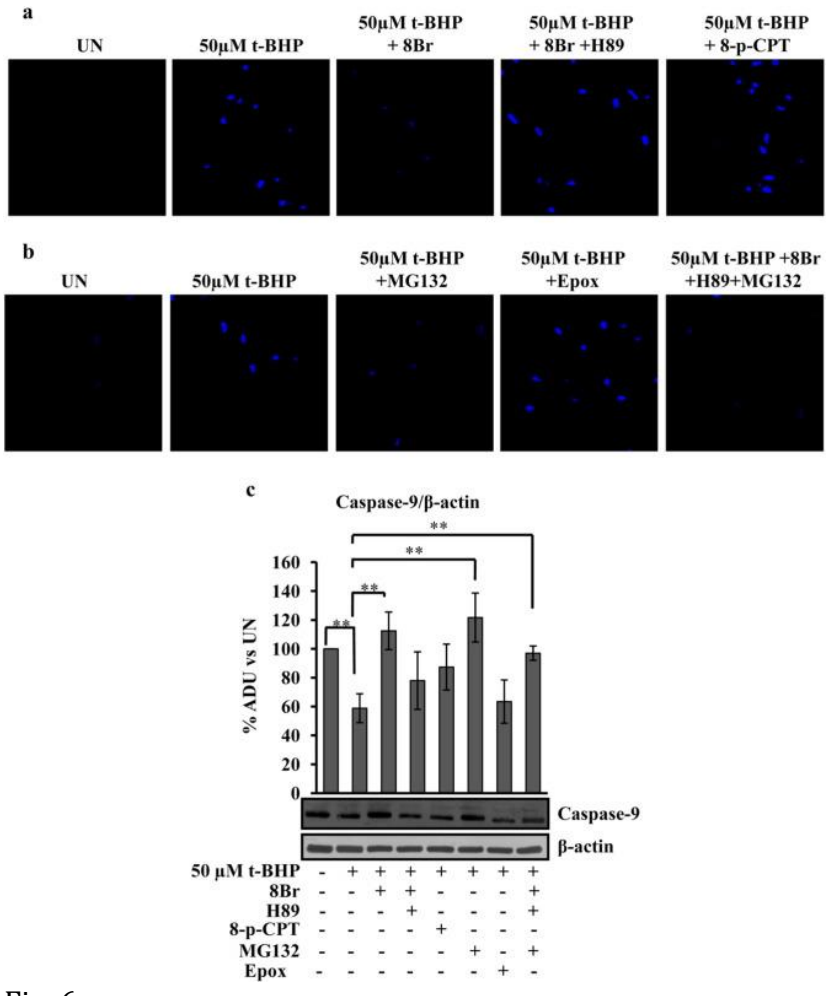
a
UN
50μM t-BHP
50μM t-BHP + 8Br
50μM t-BHP + 8Br +H89
50μM t-BHP + 8-p-CPT
b
UN
50μM t-BHP
50μM t-BHP +MG132
50μM t-BHP +Epox
50μM t-BHP +8Br +H89+MG132
c
Caspase-9/β-actin
% ADU vs UN
160
140
120
100
80
60
40
20
0
**
Caspase-9
β-actin
50 μM t-BHP - + + + + + + +
8Br - - + + - - - +
H89 - - - + - - - +
8-p-CPT - - - - + - - -
MG132 - - - - - + - +
Epox - - - - - - + -

Fig. 6

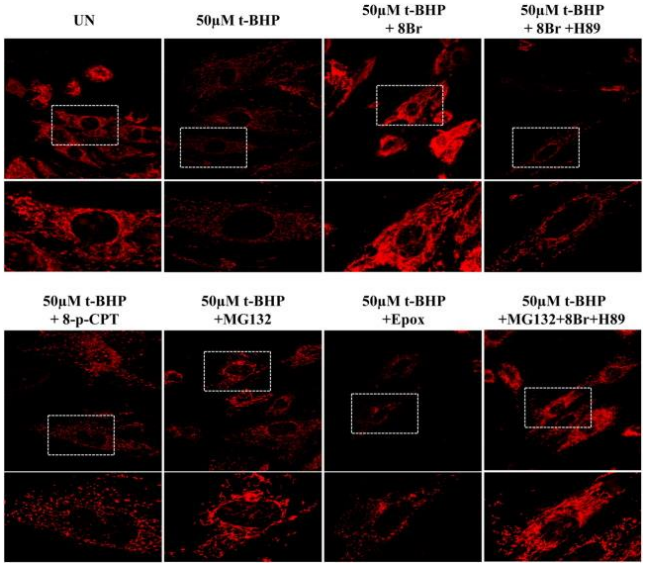
UN
50μM t-BHP
50μM t-BHP + 8Br
50μM t-BHP + 8Br +H89
50μM t-BHP + 8-p-CPT
50μM t-BHP +MG132
50μM t-BHP +Epox
50μM t-BHP +MG132+8Br+H89

Fig. 7

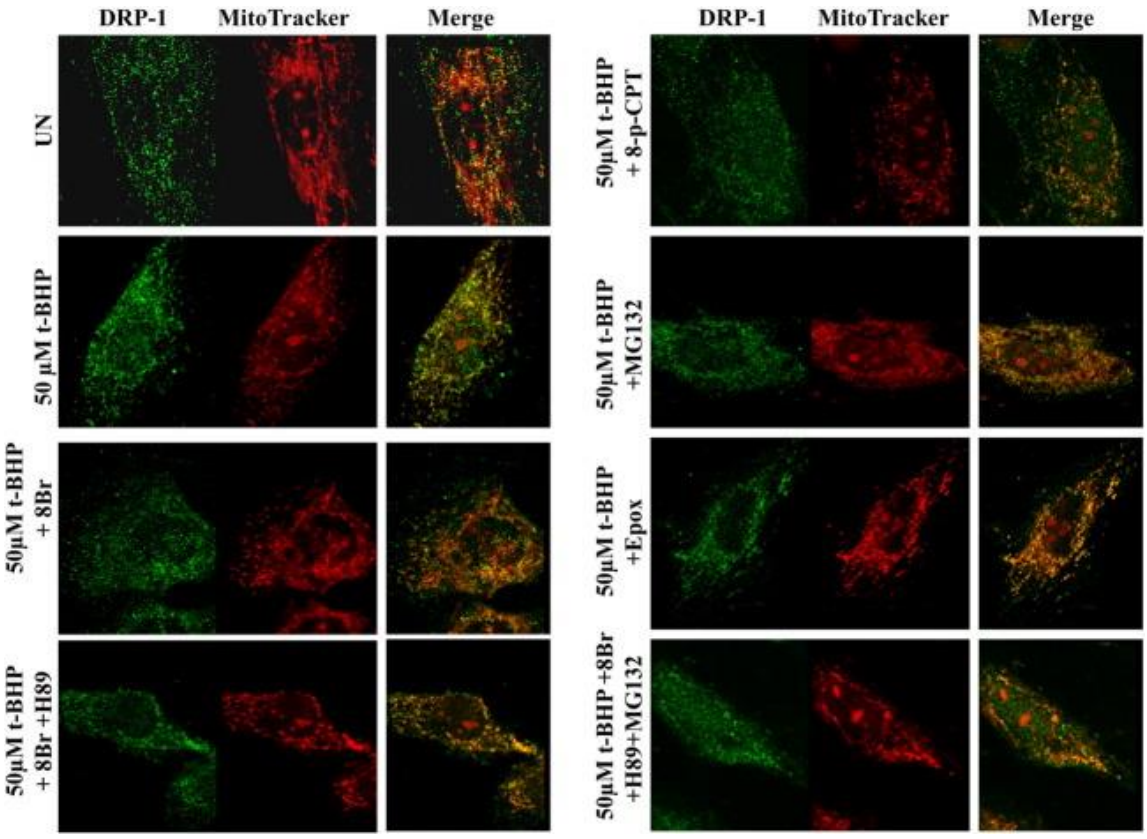

Fig. 8

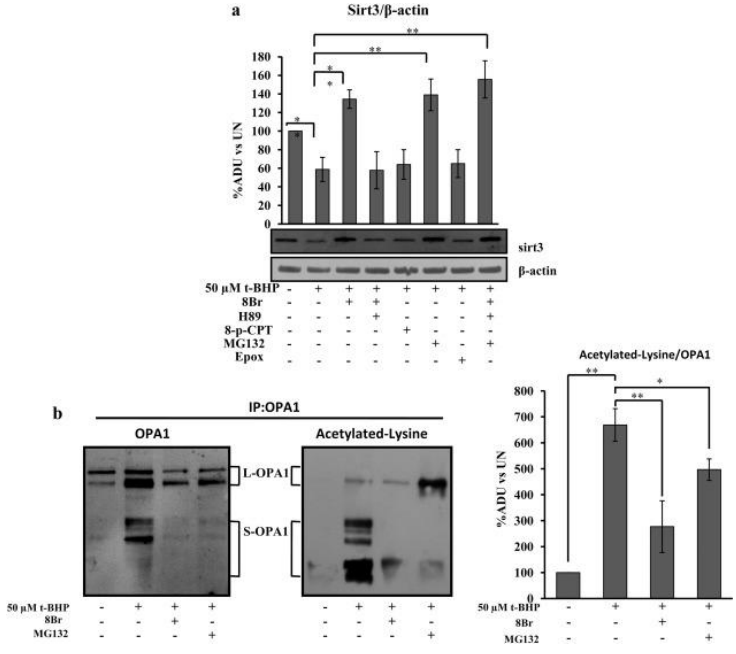

Fig. 9

Figure legends:

Fig. 1. t-BHP treatment results in increase of number of apoptotic cells, decrease of mitochondrial membrane potential and release of cytochrome *c*. Experimental conditions: the H9c2 cells were cultured in standard condition (untreated (UN)) or treated with 50 or 100 μM t-BHP. After 45 min of treatment with t-BHP, the medium was changed and the cells cultured for further 2 h, before being used for the analyses.
(a) The cytofluorimetric analysis of cells double labelled with Fluorescein Annexin V/PI, was performed to detect the percentage of apoptotic H9c2 cells untreated (UN) or treated with t-BHP. The histograms represent the means of values ± SEM (standard error of the mean) of different experiments (n = 5).
(b) Representative images by LSCM of DAPI stained cells. The analysis of intensity of fluorescence was obtained by Leica software. The histograms represent the means of values of arbitrary units of fluorescence (AUF) ± SEM of different experiments (n = 5).
(c) Representative images of mitochondrial membrane potential, monitored by confocal microscopy using the MitoTracker probe. LSCM images are shown at low and high magnification. The analysis of intensity of fluorescence was obtained by Leica software. The histograms represent the means of values of AUF ± SEM of different experiments (n = 5).
(d) Representative images by LSCM of immunofluorescence obtained probing H9c2 cells with MitoTracker and antibody against cytochrome *c*.

Fig. 2. t-BHP treatment results in DRP-1 translocation, decrease of caspase-9, Bad and Sirt3 protein levels and processing of OPA1. For experimental conditions see Fig. 1. (a) Representative images by LSCM of immunofluorescence of H9c2 cells probed with MitoTracker and immunostained with antibody against DRP-1. (b–d) Proteins of cellular lysate were loaded on 8% SDS-PAGE, transferred to nitrocellulose membranes and immunoblotted with the antibodies indicated in the figure. Protein loading was assessed with the β-actin antibody. The histograms of caspase-9 (b), BAD (b) and Sirt3 (d) represent the percentage changes with respect to the arbitrary densitometric units (ADU) of untreated H9c2 cells (UN). The histograms of OPA1 (c) represent the percentage of ADU of L and S forms of OPA1 in each lane. The values are means ± SEM of different experiments (n = 5), *p < 0.05, **p < 0.01. Student's *t*-test. For other details see under Materials and methods.

Fig. 3. The t-BHP treatment induces decrease of mitochondrial cAMP level. (a and b) H9c2 cells were transfected (transiently) with the EPAC-based FRET sensor target to cytosol (H96) or specifically to mitochondria (4mtH30). After 24 h, where indicated the cells were treated for 45 min with t-BHP at 50 or 100 μM. The FRET analyses were performed at the time indicated. The histograms represent the means values ± SEM of net% FRET observed in different experiments (n = 4), *p < 0.05. Student's *t*-test. For other details see under Materials and methods.

Fig. 4. 8-Br-cAMP prevents apoptosis in H9c2 cell cultures. Experimental conditions: the H9c2 cells were cultured in standard condition (untreated (UN)) or treated with 50 or 100 μM t-BHP as described in the legend to Fig. 1. Where indicated, before of t-BHP treatments, the cells were treated for 30 min with 100 μM 8-Br-cAMP (8Br) or 1 μM isoproterenol (ISO) then the medium was changed and t-BHP treatment performed as described above. (a) Representative images of LSCM of DAPI stained cells. The analysis of intensity of fluorescence was obtained by Leica software. The histograms represent the means values of AUF ± SEM of different experiments (n = 5). Student's *t*-test. (b) The cytofluorimetric analysis of cells double labelled with Fluorescein Annexin V/PI, was performed to detect the percentage of apoptotic H9c2 cells treated with 8-Br-cAMP + t-BHP with respect to t-BHP at concentration indicated. The histograms represent the means of values ± SEM of different experiments (n = 5). (c) Representative images of mitochondrial membrane potential, monitored by confocal microscopy using the MitoTracker probe. LSCM images are shown at low and high magnification. (d) Proteins of cellular lysate were loaded on 8% SDS–PAGE, transferred to nitrocellulose membranes and immunoblotted with the antibodies against caspase-9 or BAD. Protein loading was assessed with the β-actin antibody. The histograms represent the percentage changes with respect to the ADU of untreated H9c2 (UN). The values are means ± SEM of different experiments (n = 5), *p < 0.05, **p < 0.01. Student's *t*-test. For other details see under Materials and methods.

Fig. 5. 8-Br-cAMP prevents the appearance of S-OPA1 form and the decrease of Sirt3 protein level. For experimental conditions see legends to Fig. 1, Fig. 4. (a, b) Proteins of cellular lysate were loaded on 8% SDS–PAGE, transferred to nitrocellulose membranes and immunoblotted with the antibodies against OPA1 and Sirt3. Protein loading was assessed by reprobing the blots with the β-actin antibody. (a) The histograms represent the percentage of ADU of L and S forms of OPA1 in each lane. (b) The histograms represent the percentage changes with respect to the ADU of untreated H9c2 (UN). The values are means ± SEM of different experiments (n = 4), *p < 0.05, **p < 0.01. Student's *t*-test. For other details see under Materials and methods.

Fig. 6. cAMP/PKA signaling and mitochondrial protease inhibitor prevent DAPI staining and proteolysis/activation of caspase-9. Experimental conditions: the H9c2 cells were cultured in standard condition (untreated (UN)) or treated with 50 μM t-BHP. After 45 min of treatment with t-BHP, the medium was changed and the cells cultured for further 2 h, before being used for the analyses. Where indicated, before of t-BHP treatment, the cells were treated for 30 min with 100 μM 8-Br-cAMP (8Br) or 8Br plus 5 μM H89 or 100 μM 8-pCPT-2′-O-Me-cAMP (8-pCPT) or 10 μM MG132 or 5 μM Epoxomicin (Epox) or 8Br plus H89 plus MG132, then the medium was changed and t-BHP treatment performed as described above. (a and b) Representative images of LSCM of DAPI stained cells. (c) Proteins of cellular lysate were loaded on 8% SDS–PAGE, transferred to nitrocellulose membranes and immunoblotted with the antibody against caspase-9. Protein loading was assessed by the β-actin antibody. The histograms represent the percentage changes with respect to the ADU of untreated H9c2 (UN). The values are means ± SEM of different experiments (n = 5), *p < 0.05, **p < 0.01. Student's *t*-test. For other details see under Materials and methods.

Fig. 7. cAMP/PKA signaling and MG132 prevent the decrease of mitochondrial membrane potential and mitochondrial fragmentation. For experimental conditions see the legend to Fig. 6. Representative images of mitochondrial membrane potential, monitored by confocal microscopy using the MitoTracker probe. LSCM images are shown at low and high magnification.

Fig. 8. Effect of cAMP/PKA signaling and MG132 on DRP-1 mitochondrial translocation. For experimental conditions see the legend to Fig. 6. Representative images by LSCM of immunofluorescence of H9c2 cells probed with MitoTracker and immunostained with antibody against DRP-1.

Fig. 9. cAMP/PKA signaling and MG132 prevent the decrease of protein level of Sirt3 and control the acetylation of OPA1 (a) For experimental conditions see the legend to Fig. 6. Proteins of cellular lysate were loaded on 8% SDS–PAGE, transferred to nitrocellulose membranes and immunoblotted with the antibody against Sirt3. Protein loading was assessed by immunoblotting with the β-actin antibody. The histograms represent the percentage changes with respect to the ADU of untreated H9c2 (UN). The values are means ± SEM of different experiments (n = 4). (b) Experimental conditions: the H9c2 cells were cultured in standard condition (untreated (UN)) or treated with 50 μM t-BHP. After 45 min of treatment with t-BHP, the medium was changed and the cells cultured for further 2 h, before being used for the analyses. Where indicated, before of t-BHP treatment, the cells were treated for 30 min with 8-Br-cAMP (8Br) or MG132, then the medium was changed and t-BHP treatment performed as described above. Proteins of cellular lysate were immunoprecipitated with antibody against OPA1, loaded on 8% SDS–PAGE, transferred to nitrocellulose membranes and immunoblotted with the antibodies against OPA1 and acetylated-lysine. The histograms represent the percentage changes with respect to the ADU of untreated H9c2 (UN). The values are means ± SEM of different experiments (n = 3), *p < 0.05, **p < 0.01. Student's *t*-test. For other details see under Materials and methods.